Flood susceptibility assessment using extreme gradient boosting (EGB), Iran

Sajjad Mirzaei[1, 2], Mehdi Vafakhah[*1], Biswajeet Pradhan[3, 4] and Seyed Jalil Alavi[1]

Sajjadmirzaei@modares,ac.ir

*Corresponding author: E-mail address: VAFAKHAH@modares.ac.ir

Biswajeet.Pradhan@uts.edu.au and Biswajeet24@gmail.com

j.alavi@modares.ac.ir

1-Natural Resources and Marine Sciences, Tarbiat Modares University, 46417-76489 11 Noor, Mazandaran, Iran

2- Guest Researcher, Department of Agricultural Sciences, University of Naples Federico II, Italy.

3- The Centre for Advanced Modelling and Geospatial Information Systems (CAMGIS), Faculty of Engineering and Information Technology, University of Technology Sydney, Ultimo, New South Wales 2007, Australia; Email. Biswajeet.Pradhan@uts.edu.au (B.P.)

4- Department of Energy and Mineral Resources Engineering, Sejong University, Choongmu-gwan, 209, Neungdong-roGwangin-gu, Seoul 05006, Korea; Email. Biswajeet24@gmail.com

Abstract

Flood occurs as a result of high intensity rainfall, long-term rainfalls and snowmelt which flows out of the main river channel onto the floodplain areas and damages to buildings, roads, and facilities and causing life losses. This study aims to implement Extreme gradient boosting method for the first time in flood susceptibility modelling and compare its performance with three advanced benchmark models including Frequency Ratio (FR), Random Forest (RF), and Generalized Additive Model (GAM). The input factors include altitude, slope, plan curvature, profile curvature, stream power index (SPI), topographic wetness index (TWI), distance from rivers, normalized difference vegetation index (NDVI), rainfall, land use, and lithology. For running the models, 243 flood locations were detected by field surveys and national reports. The same number of locations were randomly created in the study regions and considered as non-flood locations. Both flood and non-flood locations were fed into the models and output flood susceptibility maps were produced. To evaluate the efficacy of the algorithms, receiver operating characteristics (ROC) curve were implemented. The results of the current research showed that the RF model and EGB had the best performances with the area under ROC curve (AUC) of 0.985, and 0.980, followed by the GAM and FR model with AUC values of 0.97, and 0.953, respectively.

The results of factor importance by the RF model showed that distance from rivers had an important influence on flood susceptibility mapping (FSM), followed by profile curvature, slope, TWI, and altitude. Considering the high performances of the RF and EGB models in flood susceptibility modelling, application of these models is recommended for such studies.

Keywords: Flood susceptibility; GIS; Generalized additive model; extreme gradient boosting; Iran

1. Introduction

Flood is defined as a natural disaster that affects different areas worldwide in humid, semi-arid, and arid regions (Addabbo et al. 2016). Thus, this phenomenon causes a huge number of deaths and much damages to the cities (Bathrellos et al. 2016). In the recent past, floods have occurred more frequently as a result of climate changes like the variations in air temperature and rainfall amount and intensity. Apart from the increase of the flood frequency, inappropriate land use planning and management has enhanced both damages costs and life losses. To manage the situation and decrease the damages or even forbid them, it is essential to first determine flood-prone areas (Lee et al. 2017).

Regarding the complicated hydrological features of the Watershed and the ever-increasing anthropogenic impacts, floods are hard to be modelled implementing simple non-linear algorithms (Khosravi et al. 2018). For this reason, machine learning and statistical models have been implemented for flood prediction because of their higher efficiency (Tien et al. 2019). Some examples of these models are: artificial neural networks (Sahoo, Ray, and De Carlo 2006; Youssef, Pradhan, and Hassan 2011), support vector machines (Shafapour et al. 2015), logistic regression (Nandi et al. 2016), evidential belief function and decision trees (Rahmati and Pourghasemi 2017), frequency ratio (Rahmati, Pourghasemi, and Zeinivand 2016) random forest and boosted-tree (Lee et al. 2017), Genetic Algorithm Rule-Set Production (GARP) and Quick Unbiased Efficient Statistical Tree (QUEST) (Darabi et al. 2019), weakly labeled support vector machine (WELLSVM) (Zhao et al. 2019), Reducederror pruning trees (REPTree) with Bagging (Bag-REPTree) and Random subspace (RS-REPTree) ensemble frameworks (Chen et al. 2019), classification and regression trees and alternating decision tree (Janizadeh et al. 2019), and alternating decision tree (ADT), functional tree (FT), kernel logistic regression (KLR), multilayer perceptron (MLP) and quadratic discriminant analysis (QDA) (Janizadeh et al. 2019). Additionally, some other studies indicated that hybrid models, such as ensemble of Decision Tree, weights-of-evidence and support vector machines (Tehrany et al. 2014; Tehrany, Jones, and Shabani 2019), neuro-fuzzy system integrated with metaheuristic algorithms (Termeh et al. 2018; Tien Bui et al. 2016), logistic model tree with bagging ensembles (Chapi et al. 2017), swarm optimized neural networks (Ngo et al. 2018), RF,ANN, SVM (Zhao et al. 2018), ensemble of evolutionary models and ANFIS (Hong et al. 2018), ensemble of multivariate discriminant analysis, CART, and SVM (Choubin et al. 2019), ensemble of multi-criteria decision making (Wang et al. 2019), fuzzy rule based ensembles (Bui et al. 2019), ensemble of RF, Stochastic Gradient Boosted Model, and Extreme Learning Machine (Shin et al. 2019), had better performances than their single models. Investigating the literature refers that different kinds of algorithms have been used for modelling flood susceptibility, but there still need to use newer and more advanced models to find the best solution to control flood disaster regarding its complicated behaviour. Therefore, this study aims to model flood susceptibility by the new model EGB and compare its performance with three benchmark models i.e., FR, RF, and GAM. The FR, RF, and GAM models have been successfully implemented in flood susceptibility modelling and different other fields of spatial assessment such as groundwater potential mapping (Golkarian et al. 2018; Motevalli et al. 2019; Naghibi et al. 2019; Rahmati et al. 2016) as well as landslide (Dou et al. 2019; Hong et al. 2019), gully, and forest fire susceptibility mapping (Gigović et al. 2019). Therefore, the main novelty of this research is the application of the EGB in flood susceptibility mapping (FSM). The fundamental advantage of the EGB is the implementation of the boosting method, which produces strong predictions by “combining several weak learners”. Application of the EGB can diminish the impact of “over-fitting issue” in the final model and produce more generalized outputs.

2. Material and Methods

This study first determines flood locations based on field surveys and national reports. Additionally, non-flood locations are produced with a “random-systematic” strategy. Then, we prepare the flood conditioning factors and classify them into training and validation datasets. These datasets are used in order to model flood susceptibility. The output susceptibility maps are validated by Accuracy, and Kappa indices as well as ROC curve. A detailed methodology flow chart is shown in Fig. 1.

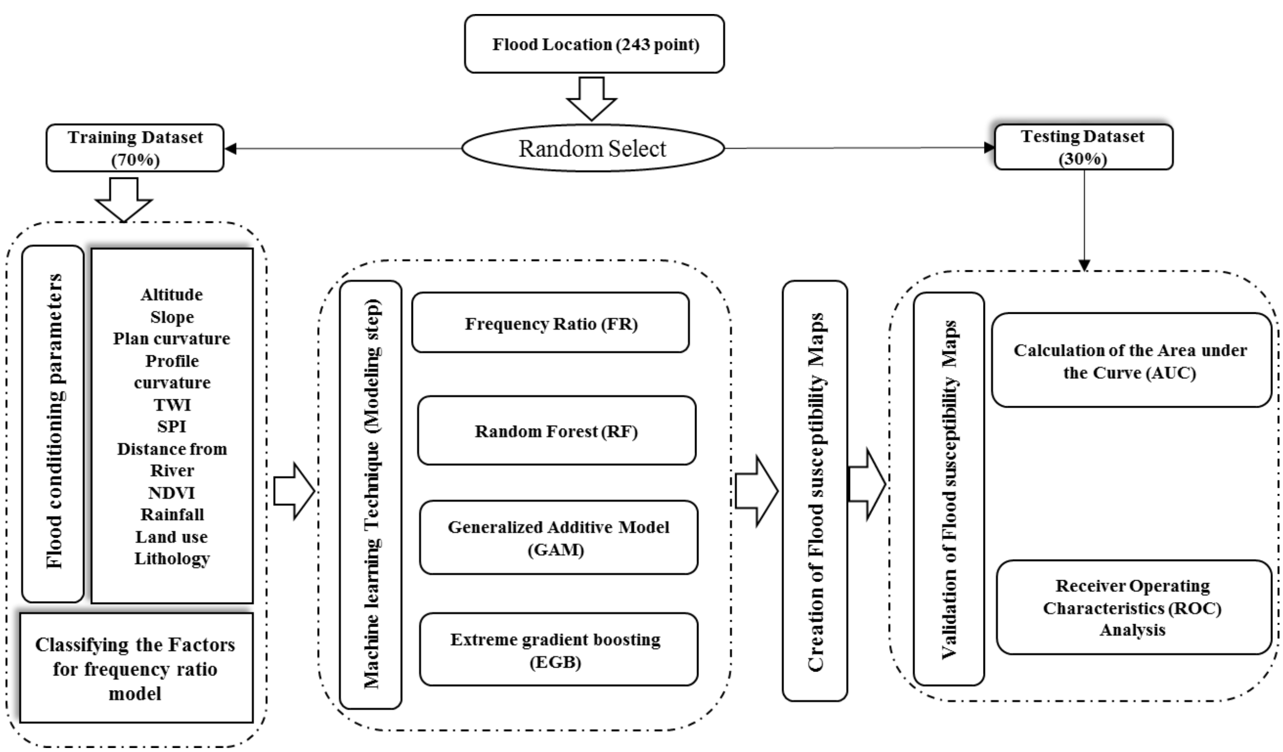

Fig. 1 Flowchart of the methodology in the current study.

2.1. Study area

The study area has an area of about 1,765 km^2. The elevation in the Talar River Watershed differs from 221 to 3,944m with an average value of 1,966m. The average width of the Talar River at the outlet of the basin is about 25.5m (Fig. 2). The investigations of (Yousefi et al. 2017) showed that this river has been impacted by floods in the past years. There are different land-use classes in the Talar Watershed including bare land, agriculture, forest, rangeland, and residential areas (Fig. 3).

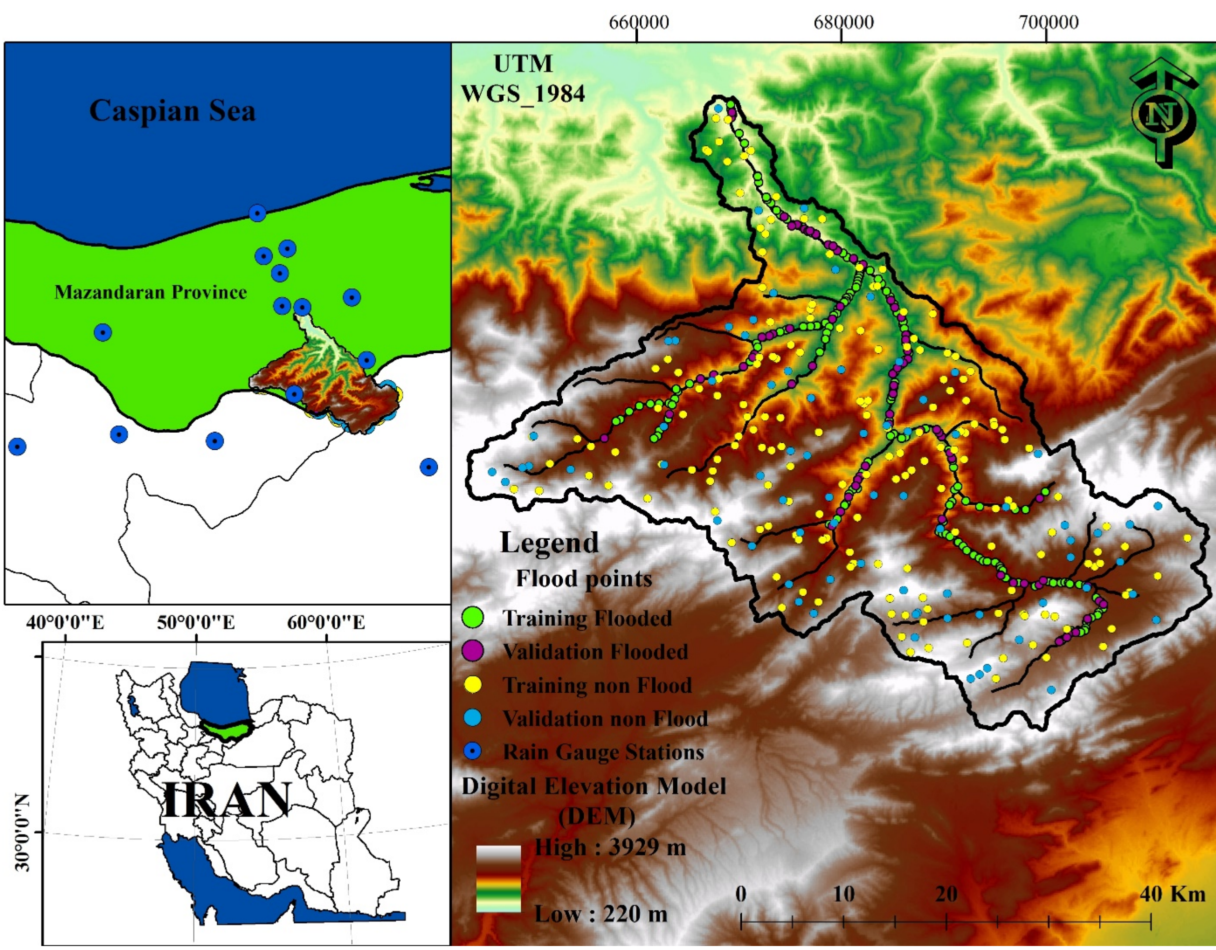

Fig. 2 Location of the study area in Iran, Mazandaran province, and location of the training (flood and non-flood) and validation (flood and non-flood).

Fig. 3 Photos were taken at four different flood affected locations in Talar watershed (photo by Sajjad Mirzaei, Zirab City).

2.2. Flood dataset

In order to detect flood locations in the Talar Watershed, several field surveys were carried out to detect flood marks in lowland areas of the watershed. In addition, hydrology and flood reports as well as the findings of (Motevalli and Vafakhah 2016; Yousefi et al. 2017) were used. Overall, 243 flood locations were detected in the study area. In order to apply the machine learning models, which need non-occurrence or in this study non-flood locations, 243 locations were systematic-randomly selected. First, the points were generated in ArcGIS, and then were investigated in order to check whether they have been selected correctly. Then, flood and non-flood locations were categorized into groups of training and validation covering 70 and 30% of the points, respectively (Fig. 2).

2.3. Flood conditioning factors

This study considered several flood susceptibility conditioning factors based on the literature (Hong et al. 2018; Khosravi et al. 2018; Rahmati et al. 2016; Shafapour et al. 2015; Tehrany et al. 2014; Termeh et al. 2018) and data availability. The input factors include altitude, slope, plan curvature, profile curvature, stream power index (SPI), topographic wetness index (TWI), distance from rivers, normalized difference vegetation index (NDVI), rainfall, land use, and lithology.

The altitude of the study region was obtained from the ASTER-Global digital elevation model (DEM) having a 30*30m spatial resolution. Altitude determines the level of drainage development in an area. Generally, higher altitudes have high river density and low discharge, while the situation is different in lowland areas. Altitude in the study basin ranges from 221 to 3,944 m (Fig. 4a). Slope impacts of water flow velocity over the ground surface and in the channels. This factor was calculated using DEM and is presented in Figure 5b. The study area has slopes ranging from 0 to 69 degrees. Plan and profile curvature were created using the DEM of the study region and used in the modelling process (Fig. 4c). These curvatures influence the water flow velocity as well as erosion and deposition processes (Fig. 4d).

SPI presents the river strength for the erosion process. SPI has a direct influence on flood occurrence because it increases with slope and upland Watershed area (Lee et al. 2018).

SPI can be computed as follows (Dewan and Yamaguchi 2008) (Fig.5e):

$$SPI = As \times \tan b \tag{1}$$

where, As depicts certain basin area, and b slope degree at each point of the basin.

TWI can be calculated as follows (Beven and Kirkby 1979) (Fig. 4f):

$$TWI = \ln\left(\frac{a}{\tan b}\right) \tag{2}$$

where, a is the cumulative area to a specific pixel, and b is slope angle at any given pixel.

Distance from river influences the discharge and spread of the flooding in a given area (Glenn et al. 2012; Wan, Lei, and Chou 2010). Distance from river layer was created by the Euclidean distance function in ArcGIS 10.2 (Fig. 4g).

Land use and NDVI are indicators of land cover in an area. Land use was created by a "supervised learning algorithm" which is a common way of classifying land use (Alganci et al. 2013; Basukala et al. 2017; Kantakumar and Neelamsetti 2015; Myint et al. 2011; Thakkar et al. 2017). The Talar River Watershed was classified into five classes of rangeland, agriculture, forest, residential areas and barren lands (Fig. 4h). Vegetated parts of the watershed have a lower susceptibility to flood incidence because there is a reverse relationship between flooding incidence probability and vegetation cover (Tehrany, Pradhan, and Jebur 2013). NDVI was computed regarding the red and infrared bands of an image on 2 July 2017 (Row: 35, Path: 163) from Landsat OLI-IRS.

Rainfall data were obtained from 14 rainfall and climatology stations in and around the study region (Table 1). in this study Universal and ordinary Kriging and Co-kriging interpolation methods were evaluated by circular, spherical, exponential, Gaussian, Stable, J-Bessel, K-Bessel, Hole Effect, Rational Quadratic models and Inverse Distance Weighting (IDW), Radial Basis Function (RBF), Global Polynomial Interpolation (GPI), Local Polynomial Interpolation (LPI), General and local estimators using Arc GIS software.

Table 1 Average annual rainfall at the rain-gauge stations, their location and height

Station name	Average annual rainfall (mm)	Latitude	Longitude	Height (m)
Talar	1032	36° 18'	52° 46'	102
Babol	668	36° 31'	52° 40'	0
Vastan	614	36° 20'	53° 9'	378
Shirgah	1033	36° 17'	52° 53'	270
Kiakola	677	36° 33'	52° 48'	-5
Sangdeh	853	36° 3'	53° 13'	1337
Babolsar	896	36° 43'	52° 39'	-21
Gharakhil	559	36° 27'	52° 46'	14.7
Doshan Tappeh	264	35° 42'	51° 20'	1209.2
Abali	537	35° 45'	51° 53'	2465.2
Firouzkooh	290	35° 55'	52° 50'	1975.6
Semnan	145	35° 35'	53° 33'	1130.8
Firouzkooh bridge	412	35° 43'	52° 24'	2985.7
Baladeh	304	36° 12'	51° 48'	2120

After performing the interpolation operation by geostatistical and deterministic methods for comparing, evaluating and selecting suitable interpolation method of five statistical parameters of Maen Error (ME), Root Mean Square (RMS), Average Standard Error (ASE), Mean Standardized (MS) and Root Mean Square Standard (RMSS) were used (Eq. (1, 2 , 3, 4 and5)).

$$\mathrm{MAE} = \frac{1}{\mathrm{n}} \sum_{\mathrm{i=1}}^{\mathrm{n}} \left| \mathrm{Q_i} - \mathrm{Q_m} \right| \tag{1}$$

$$\mathrm{RMSS} = \frac{1}{\mathrm{n}} \sum_{\mathrm{i=1}}^{\mathrm{n}} \mathrm{RMSE}_i \tag{2}$$

$$\mathrm{RMSE} = \sqrt{\frac{\sum(\mathrm{Q_i} - \mathrm{Q_m})^2}{\mathrm{n}}} \tag{3}$$

$$\mathrm{MS} = \frac{\sum(\mathrm{Q_i} - \mathrm{Q_m})}{SD} \tag{4}$$

$$\mathrm{ASE} = \frac{1}{\mathrm{n}} \sum SE \tag{5}$$

In which SE (standard error) ($\frac{\mathrm{SD}}{\sqrt{n}}$), SD (Standard deviation), Qi (observations), Qm (Estimated) and i = 1, ..., n where n is the number of observational data.

In each method, the lowest rank was devoted to the lowest statistical error and the highest rank was devoted to the highest statistical error, and then sum of the ranks was used to compare the interpolation methods (Table 2).

Table 2 Selected of the best model in interpolation methods.

Interpolation method	Model	ASE	RMSS	MS	RMS	Mean	Rank	Select
Co-Kriging (Correlation with latitude) (R=0.65)	Circular	218.84	1.3426	0.093	279.47	45.54	31	
		7	5	8	6	5		
	Spherical	221.81	1.3210	0.084	279.16	42.32	27	
		9	4	6	4	4		
	Tetraspherical	221.29	1.3085	0.087	278.97	41.89	23	
		10	2	5	3	3		
	Pentaspherical	218.61	1.3115	0.090	279.12	41.35	23	

		6	3	7	5	2		
	Exponential	232.76 11	1.1010 1	0.073 3	260.13 2	33.80 1	**18**	√
	Gaussian	200.74 3	6.0659 7	-0.005 1	484.98 7	126.19 7	25	
	Rational Quadratic	220.43 8	1.3830 6	0.095 9	259.05 1	48.77 6	30	
	Hole Effect	135.07 2	70.562 10	-13.05 10	1057.78 10	199.19 10	42	
	K-Bessel	203 5	9.49 9	-0.779 4	503.5 9	129.87 9	36	
	J-Bessel	109.1 1	349 11	-69.56 11	2216.2 11	262.49 11	45	
	Stable	200.7 4	6.06 8	-0.005 2	484.98 8	126.19 8	30	
Kiriging	Circular	261.42 2	1.045 9	0.069 8	270.46 9	34.19 9	37	
	Spherical	261.94 3	1.0469 10	0.075 10	271.58 10	36.34 10	43	
	Tetraspherical	265.33 9	0.941 6	0.0532 4	242.50 6	29.48 3	28	
	Pentaspherical	267.57 10	0.902 3	0.049 2	237.23 4	27.53 2	21	
	Exponential	262.15 4	0.946 7	0.078 11	249.8 7	37.35 11	40	
	Gaussian	269.29 11	1.032 8	0.049 1	267.76 8	27.48 1	29	
	Rational Quadratic	264.22 8	0.864 1	0.067 7	225.5 2	33.96 7	25	
	Hole Effect	262.71 5	1.0775 11	0.073 9	275.9 11	33.54 6	42	
	K-Bessel	263 6	0.907 4	0.061 5	234.15 3	32.15 5	23	
	J-Bessel	260.6 1	0.9014 2	0.052 3	220.5 1	29.82 4	**11**	√
	Stable	263.11 7	0.928 5	0.0641 6	240.17 5	32.98 8	31	
RBF	Completely Regularized Spline	-	-	-	246.62 2	46.81 3	5	
	Spline with Tension	-	-	-	249.83 3	43.07 1	**4**	√
	Multiquadric	-	-	-	264.77 4	44.97 2	6	
	Inverse Multiquadric	-	-	-	244.99 1	51.83 4	5	

	Thin Plate Spline	-	-	-	298.96 5	57.82 5	10	
LPI	Exponential	-	-	-	260.25 6	19.08 6	12	
	polynomial	-	-	-	253.45 4	8.18 4	8	
	Gaussian	-	-	-	257.22 5	11.80 5	10	
	Epanechnikov	-	-	-	250.44 2	3.66 2	4	
	quartic	-	-	-	253.18 3	7.87 3	6	
	<u>constant</u>	-	-	-	246.11 1	-1.81 1	**<u>2</u>**	√
GPI	-	-	-	-	267.86	20.22		
IDW	-	-	-	-	253.96	91.07		

Models marked with √ (bold) have the minimum error in each interpolation methods.

Results showed that, in the case of annual rainfall, ordinary kriging by J-Bessel model with the lowest ranks were the most appropriate (Table 3). Interpolation method in estimating the spatial variation of annual rainfall (Fig.6k).

Table 3 Results of comparing interpolation methods (statistical and deterministic) with annual rainfall interpolation

Comparing Interpolation method		**Model**	**ASE**	**RMSS**	**MS**	**RMS**	**Mea n**	**Ran k**	**Selec t**
(1)	Co-Kriging	Exponentia l	232	1.1	0.07	260.1	33.8	9	
			1	2	2	2	2		
	<u>Kriging</u>	**<u>J-Bessel</u>**	260	0.9	0.05	220.5	29.8	**<u>6</u>**	√
			2	1	1	1	1		
(2)	RBF	Spline with Tension	-	-	-	249.8	43	5	
						2	3		
	<u>LPI</u>	**<u>constant</u>**	-	-	-	246.1	-1.81	**<u>2</u>**	√
						1	1		
	GPI	-	-	-	-	267.8	20.2	6	
						4	2		
	IDW	-	-	-	-	253.9	91	7	

						3	4		
(1) With (2) “Final”	**Kriging**	**J-Bessel**	260.60	0.901	0.05	220.5	29	**3**	√
			-	-	-	1	2		
	LPI	constant	-	-	-	246.1	-1.8	3	
			-	-	-	2	1		

(1) comparing tow best model in interpolation Statistical methods; (2) comparing four best model in interpolation Certain methods and (1) with (2) choice the best model in interpolation Certain and statistical methods (final stage).

The lithology: of the study basin was obtained from the Geology Survey of Iran (GSI) (1997).

Lithology impacts on soil permeability and has an important role in flooding and its magnitude.

There are 26 different lithology classes in the study region (Table 4; Fig, 6j).

Table 4 Lithological characteristics of the study area

FID	Lithological description
1	Alternation of dolomite, limestone and shale
2	Basaltic volcanic tuff
3	Conglomerate and sandstone
4	Conglomerate, sandstone and shale with coal seams
5	Dark grey medium - bedded to massive limestone
6	Dark grey shale and sandstone
7	High level piedmont fan and valley terrace deposits
8	Light-red coarse grained, polygenic conglomerate with sandstone intercalations
9	Light grey, thin - bedded to massive limestone (LAR FM)
10	Light- red to brown marl and gypsiferous marl with sandstone intercalations
11	Low level piedmont fan and valley terrace deposits
12	Marl, calcareous sandstone, sandy limestone and minor conglomerate
13	Marl, gypsiferous marl and limestone
14	limestone
15	Polymictic conglomerate and sandstone
16	Red conglomerate and sandstone
17	Red marl, gypsiferous marl, sandstone and conglomerate (Upper red Fm.)
18	Thick - bedded to massive limestone

19	thick bedded grey o'olitic limestone; thin - platy, yellow to pinkish limestone with worm tracks and well to thick - bedded dolomite and dolomitic limestone
20	Thick bedded to massive, white to pinkish orbitolina bearing limestone
21	Undifferentiated limestone, shale and marl
22	Undifferentiated lower Paleozoic rocks
23	Undifferentiated unit, composed of dark red micaceous siltstone and sandstone
24	Upper cretaceous, undifferentiated rocks
25	Well - bedded to thin - bedded, greenish - grey argillaceous limestone with intercalations of calcareous shale (DALICHAI FM)
26	Well bedded green tuff and tuffaceous shale

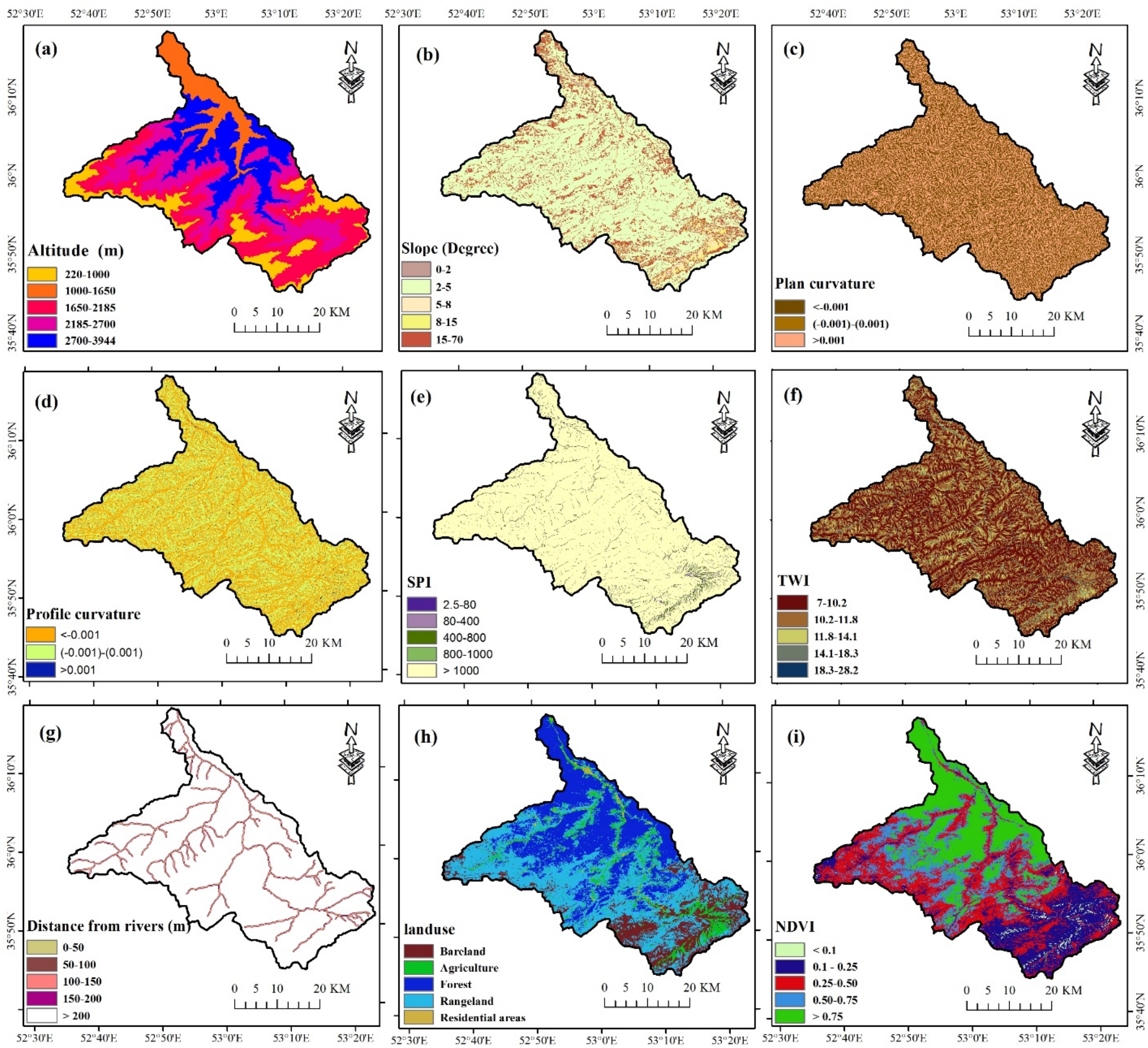

Fig. 4 Input predictor variables: (a) altitude, (b) slope angle, (c) plan curvature, (d) profile curvature, € SPI, (g) distance from the river, (h) land-use, (i) NDVI, (k) lithology, and (k) rainfall.

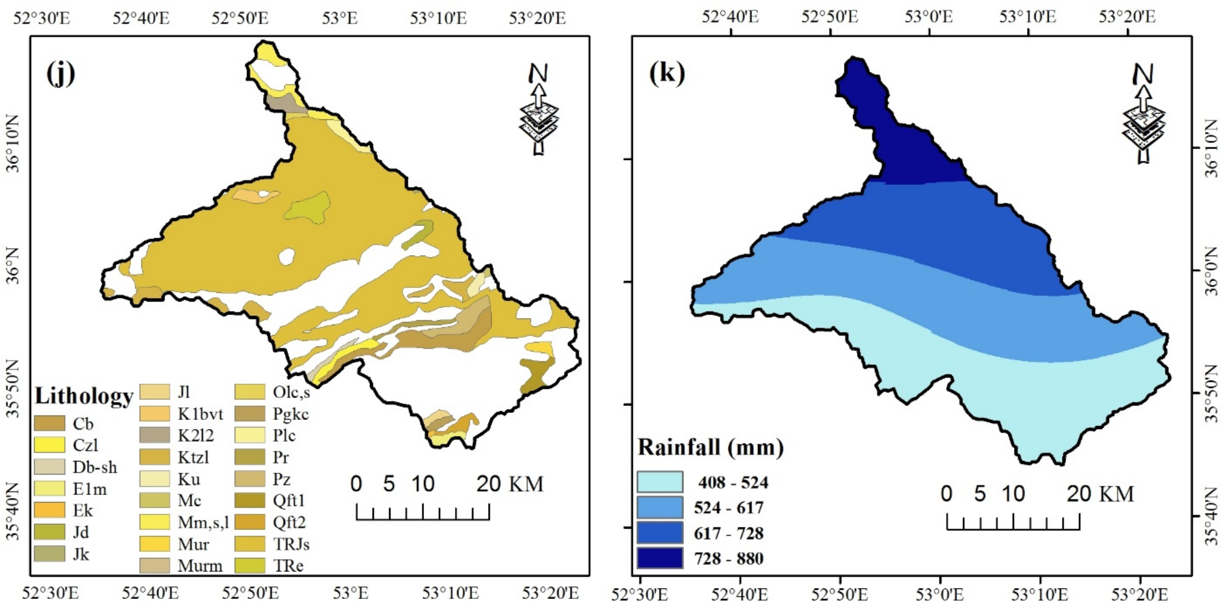

Fig. 4 continue

2.4. Classification models

2.4.1. Frequency ratio

FR was introduced by (Bonham-Carter 1994) and is explained as the probability of incidence of a specific event. This model has been used in many studies in order to define the relationship between target factors such as flood, gully, forest fire, and groundwater spring and their conditioning factors. The output of the FR is simple and helps managers and stakeholders understand the relationships between input and output factors (Nourani and Komasi 2013). FR can be calculated as below:

$$FR = \frac{F/FF}{A/AA} \quad (1)$$

where, F is the number of floods in each class, FF is the total number of floods in the study region, A is the number of pixels in each class, and AA is the total number of pixels in the study region. It is noteworthy to mention that the final FR value is obtained by summing the FR values for all factors. FR values are assigned to the pixels by "lookup" function in ArcMap and they are summed by the "weightedsum" function.

2.4.2. Random forest

RF could be regarded as an ensemble created by several decision trees as predictors and is implemented for classification and regression topics (Breiman 2001). RF is a flexible and strong algorithm that applies random trees by a set of cases through a bootstrapping method. The cases that are not considered in constructing each tree is called out of bag (Catani et al. 2013; Hong et al. 2017). There are two indices to define the contribution of the factors in RF model such as "*mean decrease accuracy and mean decrease Gini*" (Naghibi, Pourghasemi, and Dixon 2016). RF is appropriate for working with large data sets and produces satisfactory outputs (Arabameri, Pradhan, and Rezaei 2019). In RF, a voting is done between the outputs of the constructed trees and predicts the target variable, in this case, flood susceptibility. To run this model, random Forest package in R software was implemented and the maps were prepared and classified in ArcMap 10.2.

2.4.3. Generalized additive model

GAM is categorized as a "semi-parametric" regression method (Chambers and Hastie 1992; Hastie and Tibshirani 1990). Response curves of this model are predicted by smooth functions; this leads to an extensive variety of response curves to be predicted (Maggini et al. 2006;

Pourtaghi et al. 2016). An advantage of the GAM is that it could be interpreted easily, unlike other data mining, black-box, complex models (Goetz, Guthrie, and Brenning 2011). GAM is able to model non-linear features that are influenced by many factors like flood susceptibility (Petschko et al. 2014). The main difference between the generalized linear model and GAM is that the first one implements parametric impact of solitary variables, while the second one has smoother additive terms (Vorpahl et al. 2012). GAM was applied using caret and mgcv packages in R software.

2.4.4. Extreme gradient boosting

EGB method was introduced by (Chen and Guestrin 2016) is a new application of the "gradient boosting machine". The foundation of EGB is on the basis of the "boosting" which could be explained as creating a "strong learner" by combining the outputs of several "weak learners" (Fan et al. 2018). The EGB attempts to tune the parameters without making the model over-fitted. The procedure of optimization in EGB begins with creating the first learner to the whole dataset of the variables and follows with creating the next model on the residuals. The procedure finishes when it reaches "stopping criteria" (Fan et al. 2018).

3. Results and discussion

3.1. Frequency ratio

The results of the FR model are presented in Table 5. Based on the results, the highest FR is related to the elevation class of 220-1000 m with an FR value of 4.7. The class of 1000-1650 m has the second-highest FR value of 1.4. In the case of land use, it can be seen that agriculture and residential areas have the highest FR values of 7.5 and 9.7, respectively. FR for NDVI depicts that classes of less than 0.75 have high FR values. NDVI class of 0.1-0.25 and NDVI class lower than 0.1 have the highest FR values of 1.8 and 1.6, respectively. For plan curvature, the findings depicted that class of (- 0.001) - (0.001) had the highest FR value of 4.6. In the case of profile curvature, a class more than 0.001 has the highest FR value of 1.7. Rainfall classes of 725-880 and 617-728 have the highest FR values of 2.7 and 1.3, respectively. In the case of distance from rivers, it can be seen that classes of 50-100 and 150-200m have the highest FR values of 10.7 and 10.1, respectively. FR results for slope showed that classes of 0-2 (FR=5.5) and 15-70 (FR=1.3) have higher FR values than other classes. In the case of SPI, it can be seen that the class of 2.5-80 has a high FR value of 12.3. Regarding TWI, the results showed that TWI class of more than 18.3 has the highest FR value of 36.5. It should be mentioned that this class only covers one percent of the study region; thus, it does not have much importance in this model. The second highest FR value was observed for the TWI class of 14.1-18.3.

Table 5 Results of the FR model for different classes of the factors

Factor	**Class**	**Floods (%)**	**Classes area (%)**	**Frequency Ratio**
Elevation (m)	220-1000	51.9	11.1	4.7
	1000-1650	28.8	20.8	1.4
	1650-2185	15.2	25.3	0.6
	2185-2700	4.1	28.6	0.1
	2700-3944	0.0	14.2	0.0
Land use	Barren land	7.8	14.1	0.6
	Agriculture	69.5	9.2	7.5
	Forest	3.3	34.3	0.1
	Rangeland	8.2	41.2	0.2
	Residential areas	11.1	1.1	9.7
NDVI	< 0.1	2.1	1.3	1.6

	0.1 - 0.25	40.3	22.1	1.8
	0.25-0.50	39.1	30.7	1.3
	0.50-0.75	17.7	19.3	0.9
	> 0.75	0.8	26.6	0.0
Plan curvature	< -0.001	64.3	48.5	1.3
	(- 0.001) - (0.001)	5.3	1.2	4.6
	> 0.001	30.1	50.3	0.6
Profile curvature	< -0.001	7.8	46.4	0.2
	(- 0.001) - (0.001)	1.6	1.2	1.4
	> 0.001	90.6	52.4	1.7
Rainfall (mm)	408 - 524	17.7	33.4	0.5
	524 - 617	26.8	33.5	0.8
	617 - 728	32.5	24.6	1.3
	728 - 880	23.0	8.5	2.7
Distance from the rivers (m)	0-50	15.2	3.7	4.2
	50-100	25.5	2.4	10.7
	100-150	14.4	2.8	5.2
	150-200	23.9	2.4	10.1
	> 200	21.0	88.7	0.2
Slope (degree)	0-2	2.5	0.5	5.5
	2-5	2.9	2.5	1.2
	5-8	0.8	4.2	0.2
	8-15	0.8	18.5	0.0
	15-70	93.0	74.3	1.3
SPI	2.5-80	0.2	0.2	12.3
	80-400	1.8	1.8	1.6
	400-800 400-800	3.5	3.5	0.2
	800-1000	2.0	2.0	0.4
	> 1000	92.5	92.5	1.0
TWI	7-10.2	4.5	43.3	0.1
	10.2-11.8	23.5	37.4	0.6
	11.8-14.1	20.6	14.0	1.5
	14.1-18.3	14.4	4.3	3.3

	18.3-28.2	37.0	1.0	36.5

Table 6 Area percent of flood susceptibility classes for the FR, GAM, RF and EGB algorithms

Class	FR	GAM	RF	EGB
Low	72.9	90.4	77.6	91
Moderate	19	0.7	14.2	2.2
High	7	0.9	4.3	1.7
Very high	1.1	8.0	3.9	5.1

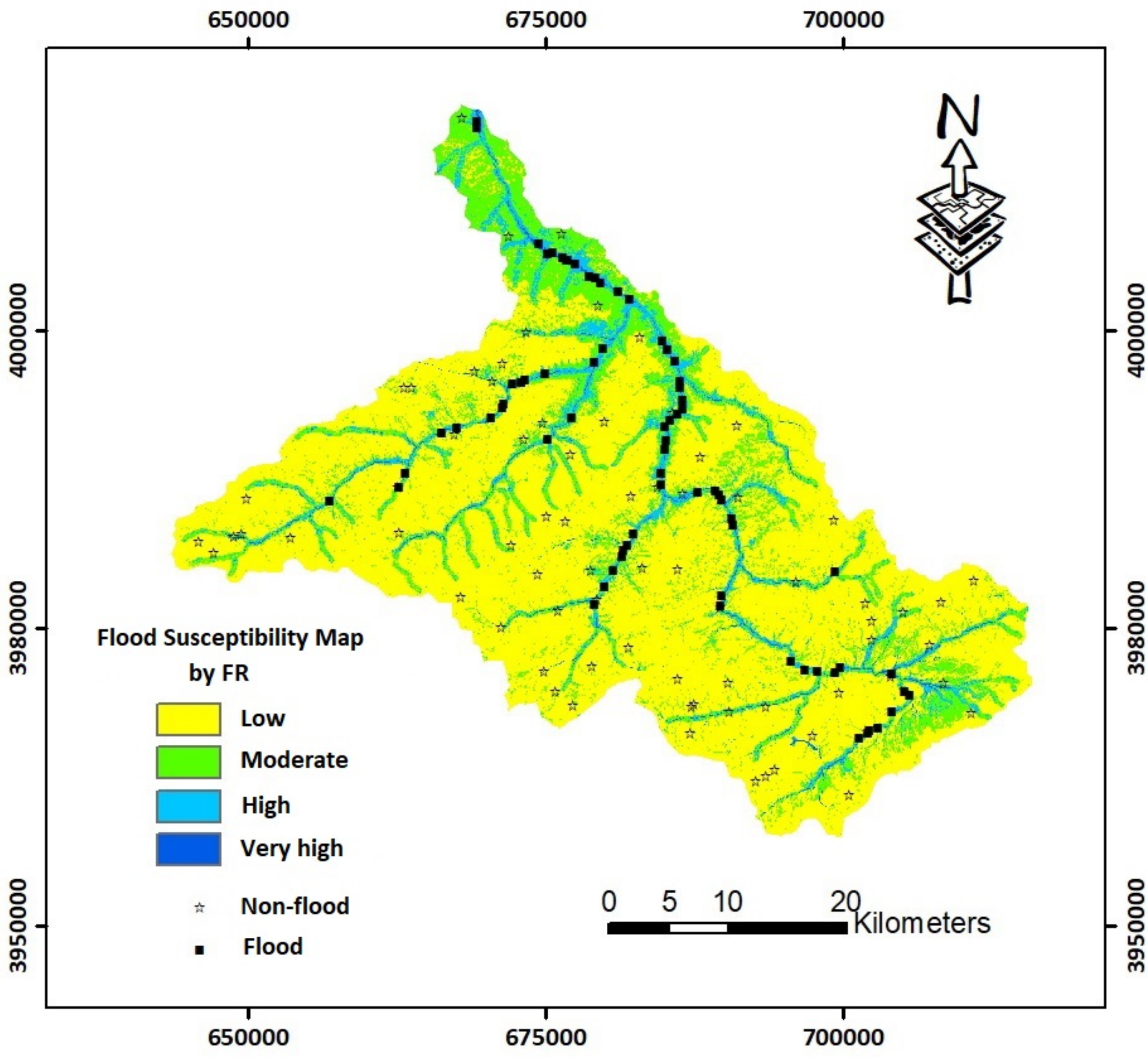

Fig. 6 Flood susceptibility map obtained by the FR algorithm

3.2. Random forest

The RF model was optimized for the training dataset with a node size of 3, mtry of 2, and 1000 trees. The confusion matrix for predictions of the RF on training data is shown in Table 7. Based on Table 8, the RF has predicted 161 non-flood cases and 164 flood cases correctly, while 10 non-floods and 5 floods are predicted incorrectly. This leads us to a class error of 0.0584 for non-flood prediction and a class error of 0.0295 for flood prediction. The importance of the factors in flood susceptibility mapping was defined through the calculation of mean decrease Gini and is presented in Table 7. Based on the results, altitude, distance from rivers, TWI, slope, and land use had the highest importance in modelling flood susceptibility. On the contrary, lithology, NDVI, and SPI were reported to be the least important factors. Figure 9 shows the flood susceptibility map produced by the RF model. According to the flood susceptibility map, low, moderate, high, and very high susceptibility classes cover 77.6, 14.2, 4.3, and 3.9% of the study area, respectively.

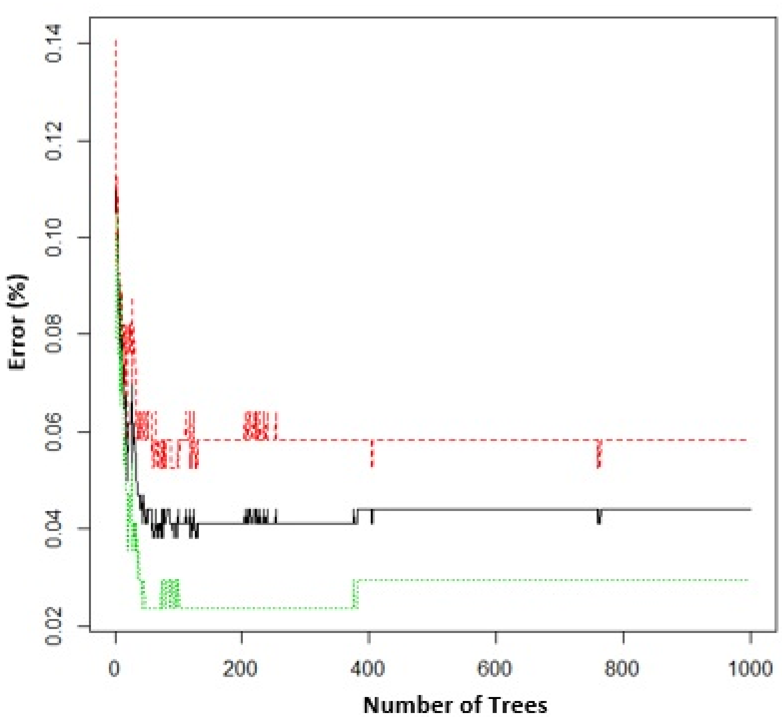

Fig. 7 Optimization results of the RF model in this study.

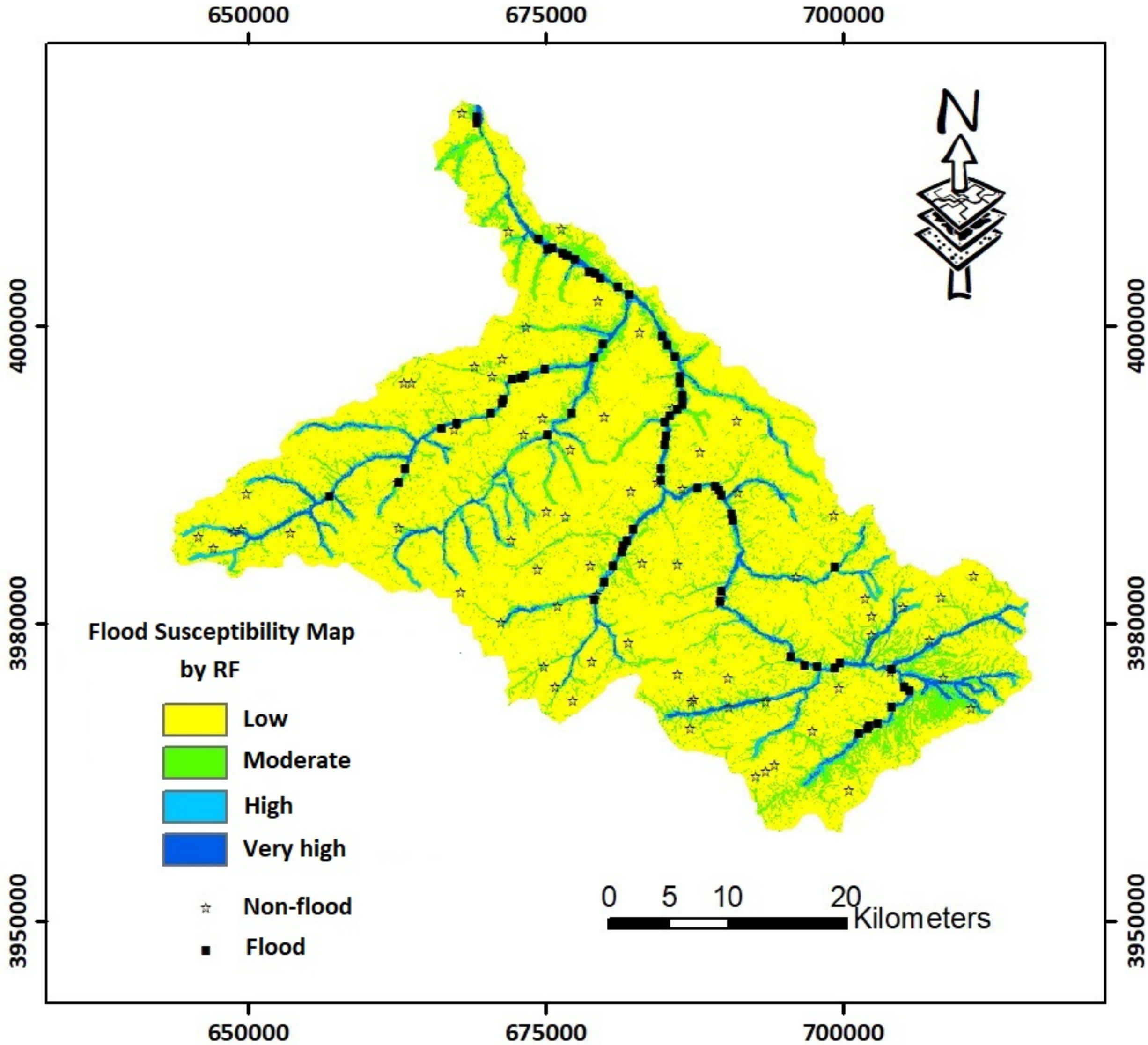

Fig. 8 Flood susceptibility map obtained by the RF algorithm

Table 7. Importance of the factors in modelling flood susceptibility in the study area

Factors	**Mean decrease accuracy**
Distance from the rivers	51.20
Profile curvature	22.61
Slope	19.35
TWI	15.76
Altitude	13.18
NDVI	10.85
SPI	9.76
Land use	9.59
Rainfall	5.77
Plan curvature	5.22
Lithology	1.28

Table 8. Confusion matrix of the RF model for the training dataset

	Non-Flood	Flood	Class error
Non-Flood	161	10	0.0584
Flood	5	164	0.0295

3.3. Generalized additive model

The GAM was optimized by a select parameter of FALSE with accuracy and Kappa indices of 0.98 and 0.97, respectively. For optimizing the GAM, the tuning parameter of the method was selected to be “generalized cross-validation Cp”. Fig. 9 shows the flood susceptibility map produced by the GAM. Based on the flood susceptibility map, low, moderate, high, and very high susceptibility classes occupy 90.4, 0.7, 0.9, and 8% of the studied region, respectively.

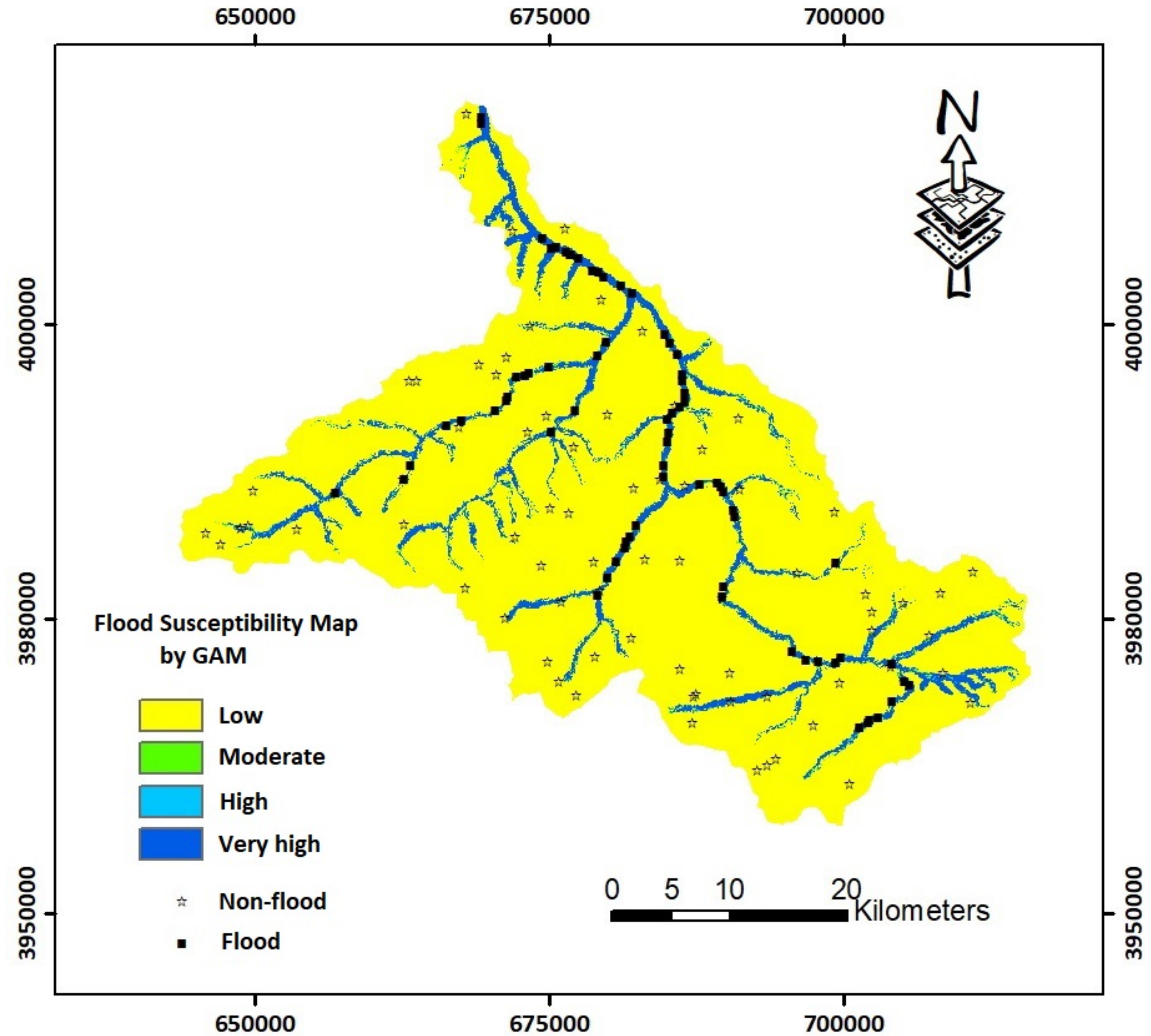

Fig. 9 Flood susceptibility map obtained by the GAM algorithm

3.4. Extreme gradient boosting

Based on the results, the final EGB model was optimized with rounds of 100, lambda of 0.1, an alpha of 0.1, and eta of 0.3. The accuracy and Kappa of the model with the mentioned parameters were calculated as 0.95, and 0.90. Low, moderate, high, and very high classes of susceptibility cover 91.6, 14.2, 4.3, and 3.9%, respectively (Fig 11).

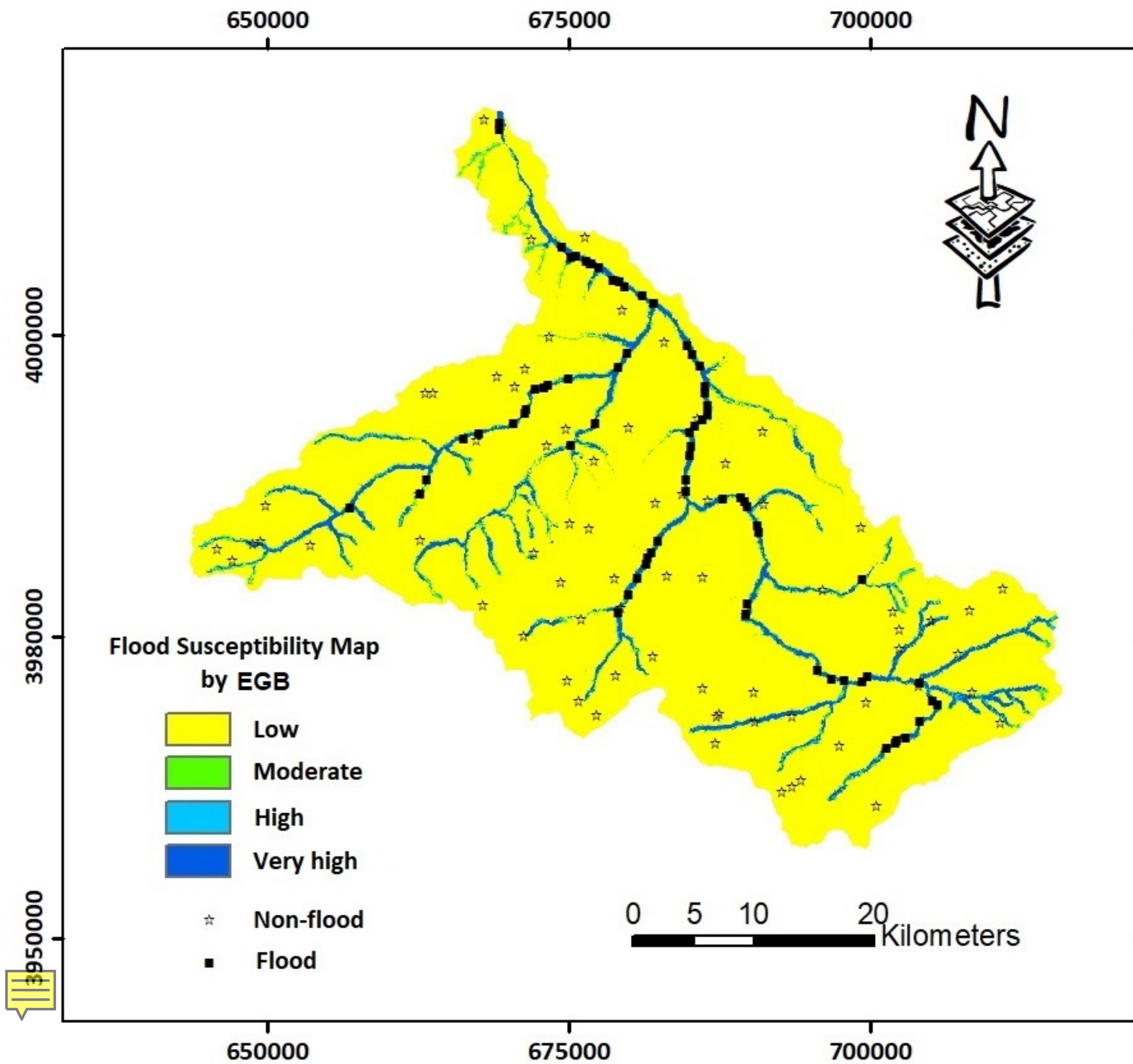

Fig. 11 Flood susceptibility map obtained by the EGB algorithm

3.5. Evaluating the performance of the models

Due to the importance of the performance evaluation step, this study used receiver operating characteristics (ROC) curve for this purpose. ROC is a common and strong method for evaluating binary issues and has been used in different fields of study including groundwater, flood, floodwater, and landslide (Golkarian et al. 2018; Kordestani et al. 2019; Naghibi, Ahmadi, and

Daneshi 2017; Naghibi, Pourghasemi, and Abbaspour 2018; Rahmati et al. 2018). ROC curve plots "sensitivity" against "1-specificity" at different cut-off values (Conoscenti et al. 2016; Naghibi and Moradi Dashtpagerdi 2016). The area under the curve (AUC) of ROC varies from 0 to 1 where an AUC close to one shows a high-performance model and an AUC close to 0 depicts a low-performance model (Hong et al. 2017; Mousavi et al. 2017; Sangchini et al. 2016). Based on the results of the ROC curve in Table 9, it can be seen that the RF and EGB are the leading models with the highest AUCs of 0.985, and 0.98, respectively. The GAM and FR models had lower accuracy than the leading models with AUC scores of 0.94 and 0.953, respectively. Based on the accuracy scores, RF had the highest performance with an accuracy of 0.965, followed by the EGB and GAM. The Kappa index also showed high performance of the RF and EGB compared to other models.

Table 9 Results of area under the ROC curve (AUC)

Test result variable(s)	AUC	Accuracy	Kappa
RF	0.985	0.965	0.931
EGB	0.98	0.9452	0.8902
GAM	0.970	0.945	0.8901
FR	0.953	0.664	0.328

3.6. Model performance comparison

The results of the current research showed that the RF and EGB had the best performance, followed by the GAM and FR algorithms. The higher performance of the RF could have resulted from its strong features. RF is robust to noise and outliers (Sameen, Pradhan, and Lee 2019), the issues that are common in geospatial works like flood susceptibility. RF is capable of predicting the importance or influence ratio of the input factors in the modeling process (Naghibi et al.

2016). This capability makes this model more interpretable than other black-box tree-based models (Pal 2005). RF is able to handle and work with multiple different inputs without an act of factor removal (Naghibi and Pourghasemi 2015; Sameen et al. 2019). RF is able to work with huge data. GAM and FR have also shown acceptable performances. FR as a statistical model provides an easy to interpret outputs that could be useful for the managers as well as stakeholders (Nourani et al. 2014). Therefore, the selected models in this study provide both complex high-performance and simple interpretable results. EGB on the other hand, applied boosting technique, which is known as a strong feature in data mining models resulting in better outputs for classification issues. This feature might have caused superior performance than two other models of GAM and FR with simpler structures. “Gradient boosting method” suffered from a lack of “strong regulation parameter”, that had made it vulnerable to “over-fitting”, but the regularization parameter in EGB makes overcomes this shortcoming (Georganos et al. 2018). The impact of boosting was also confirmed in another study i.e.,(Naghibi et al. 2017) where they used the FR model to combine the results of some data mining models. Their ensemble model constructed on the basis of boosting had better performance, which is consistent with the results of this research. The results of (Georganos et al. 2018) in object-based land-use classification proved a superior performance of the EGB comparing to other models like RF and support vector machines. The acceptable performance of the EGB in their study is in agreement with the results of this study.

The results of factor importance by the RF model showed that distance from the rivers had an important influence on flood susceptibility, followed by profile curvature, slope, TWI, and altitude. The results of (Khosravi et al. 2018) showed that altitude had the highest importance in modelling flood susceptibility, followed by distance from the river, NDVI, soil type, and slope. This shows that in spite of differences between the importances of factors affecting flood susceptibility, there are some shared results, for instance, for distance from the river, and slope. The differences between the important values in this study and (Khosravi et al. 2018) could be related to the physical, topographical, and hydrological characteristics of the Watersheds. Floods occur in certain distances from rivers; thus, this factor has had a high contribution to the modelling. Higher slopes are related to higher elevations where drainage density is higher and flood discharge is lower. Therefore, we do not expect flood occurrence in those areas. A range of slopes between mountainous and plain areas where discharge reaches higher amounts is more susceptible to flood occurrence. Profile curvature, TWI as secondary topographical factors as well as altitude impact the drainage development in different parts of the watershed, runoff speed, and erosion and sediment ratio.

4. Conclusion

Determining high susceptible areas to flood occurrence is a crucial step to manage this disaster especially in developing countries like Iran and the Middle East as data-scarce areas where there is not enough access to high quality spatial and temporal flood data. The current research develops a reliable flood susceptibility assessment for large areas confronting a lack of data through the application of the EGB model and comparing it with RF, FR, and GAM. The results depicted satisfactory efficiency of the RF and EGB models. The RF and EGB models had AUC values of more than 0.98, which is regarded as excellent prediction ability in classification issues. Thus, applications of the RF and EGB models are recommended for future studies on flood susceptibility. Further, the findings of variable importance showed a high impact of distance from the river, profile curvature, slope, TWI, and altitude in the modelling process of this phenomenon. This shows that topographical factors have a strong role in modelling flood. Researchers can obtain highly accurate flood susceptibility maps by focusing on DEM-derived factors and improving their quality. DEM-derived factors are extremely impacted by the spatial resolution of the DEM. This work suggests a step for assessing flood susceptibility of mountainous regions like Talar and provides basic information to define potentially disastrous areas and mitigate the damages. Based on the results, highly flood susceptible areas are located at the northern parts of the Talar area, which covers lowland regions. Flood control strategies and actions are suggested to be done by water resources managers for those areas.

References

Addabbo, A. D., A. Refice, G. Pasquariello, F. Lovergine, A. D'Addabbo, A. Refice, G. Pasquariello, F. Lovergine, and S. Manfreda. 2016. "Following Flood Dynamics by SAR/Optical Data Fusion." Pp. 1–5 in *2016 IEEE Workshop on Environmental, Energy, and Structural Monitoring Systems (EESMS)*. IEEE.

Alganci, Ugur, Elif Sertel, Mutlu Ozdogan, and Cankut Ormeci. 2013. "Parcel-Level Identification of Crop Types Using Different Classification Algorithms and Multi-Resolution Imagery in Southeastern Turkey." *Photogrammetric Engineering & Remote Sensing* 79(11):1053–65.

Arabameri, Alireza, Biswajeet Pradhan, and Khalil Rezaei. 2019. "Gully Erosion Zonation Mapping Using Integrated Geographically Weighted Regression with Certainty Factor and Random Forest Models in GIS." *Journal of Environmental Management* 232:928–42.

Basukala, Amit Kumar, Carsten Oldenburg, Jürgen Schellberg, Olena Dubovyk, Murodjon Sultanov, and Olena Dubovyk. 2017. “Towards Improved Land Use Mapping of Irrigated Croplands: Performance Assessment of Different Image Classification Algorithms and Approaches.” *European Journal of Remote Sensing* 50(1):187–201.

Bathrellos, G. D., E. Karymbalis, H. D. Skilodimou, K. Gaki-Papanastassiou, and E. A. Baltas. 2016. “Urban Flood Hazard Assessment in the Basin of Athens Metropolitan City, Greece.” *Environmental Earth Sciences* 75(4):1–14.

Beven, K. and M. J. Kirkby. 1979. “No Title.” *Hydrolog Sci J.* 24(null):43.

Bonham-Carter, Graeme F. 1994. “Geographic Information Systems for Geoscientists-Modeling with GIS.” *Computer Methods in the Geoscientists* 13:398.

Breiman, Leo E. O. 2001. “Random Forests.” *Machine Learning* 45(1):5–32.

Bui, Dieu Tien, Phuong-Thao Thi Ngo, Tien Dat Pham, Abolfazl Jaafari, Nguyen Quang Minh, Pham Viet Hoa, and Pijush Samui. 2019. “A Novel Hybrid Approach Based on a Swarm Intelligence Optimized Extreme Learning Machine for Flash Flood Susceptibility Mapping.” *Catena* 179:184–96.

Catani, F., D. Lagomarsino, S. Segoni, and V. Tofani. 2013. “Landslide Susceptibility Estimation by Random Forests Technique: Sensitivity and Scaling Issues.” *Natural Hazards and Earth System Sciences* 13(11):2815–31.

Chambers, John M. and Trevor J. Hastie. 1992. *Statistical Models in S*. Vol. 251. Wadsworth & Brooks/Cole Advanced Books & Software Pacific Grove, CA.

Chapi, Kamran, Vijay P. Singh, Ataollah Shirzadi, Himan Shahabi, Dieu Tien, Dieu Tien Bui, Binh Thai Pham, and Khabat Khosravi. 2017. “A Novel Hybrid Artificial Intelligence Approach for Flood Susceptibility Assessment.” *Environmental Modelling & Software* 95:229–45.

Chen, Tianqi and Carlos Guestrin. 2016. “Xgboost: A Scalable Tree Boosting System.” Pp. 785–94 in *Proceedings of the 22nd acm sigkdd international conference on knowledge discovery and data mining*. ACM.

Chen, Wei, Haoyuan Hong, Shaojun Li, Himan Shahabi, Yi Wang, Xiaojing Wang, Baharin Bin, and Baharin Bin Ahmad. 2019. “Flood Susceptibility Modelling Using Novel Hybrid Approach of Reduced-Error Pruning Trees with Bagging and Random Subspace Ensembles.” *Journal of Hydrology* 575(May):864–73.

Choubin, Bahram, Ehsan Moradi, Mohammad Golshan, Jan Adamowski, Farzaneh Sajedi-Hosseini, and Amir Mosavi. 2019. “An Ensemble Prediction of Flood Susceptibility Using Multivariate Discriminant Analysis, Classification and Regression Trees, and Support Vector Machines.” *Science of the Total Environment* 651:2087–96.

Conoscenti, Christian, Edoardo Rotigliano, Mariaelena Cama, Nathalie Almaru Caraballo-Arias, Luigi Lombardo, and Valerio Agnesi. 2016. “Exploring the Effect of Absence Selection on Landslide Susceptibility Models: A Case Study in Sicily, Italy.” *Geomorphology* 261:222–35.

Darabi, Hamid, Bahram Choubin, Omid Rahmati, Ali Torabi Haghighi, Biswajeet Pradhan, and Bjørn Kløve. 2019. “Urban Flood Risk Mapping Using the GARP and QUEST Models: A Comparative Study of Machine Learning Techniques.” *Journal of Hydrology* 569(November 2018):142–54.

Dewan, Ashraf M. and Yasushi Yamaguchi. 2008. “Effect of Land Cover Changes on Flooding: Example from Greater Dhaka of Bangladesh.” *International Journal of Geoinformatics* 4(1):11–20.

Dou, Jie, Ali P. Yunus, Dieu Tien Bui, Abdelaziz Merghadi, Mehebub Sahana, Zhongfan Zhu, Chi-Wen Chen, Khabat Khosravi, Yong Yang, and Binh Thai Pham. 2019. “Assessment of Advanced Random Forest and Decision Tree Algorithms for Modeling Rainfall-Induced Landslide Susceptibility in the Izu-Oshima Volcanic Island, Japan.” *Science of the Total Environment* 662:332–46.

Fan, Junliang, Xiukang Wang, Lifeng Wu, Hanmi Zhou, Fucang Zhang, Xiang Yu, Xianghui Lu, and Youzhen Xiang. 2018. “Comparison of Support Vector Machine and Extreme Gradient Boosting for Predicting Daily Global Solar Radiation Using Temperature and Precipitation in Humid Subtropical Climates: A Case Study in China.” *Energy Conversion and Management* 164(January):102–11.

Georganos, Stefanos, Tais Grippa, Sabine Vanhuysse, Moritz Lennert, Michal Shimoni, and Eléonore Wolff. 2018. “Very High Resolution Object-Based Land Use–Land Cover Urban Classification Using Extreme Gradient Boosting.” *IEEE Geoscience and Remote Sensing Letters* 15(4):607–11.

Gigović, Ljubomir, Hamid Reza Pourghasemi, Siniša Drobnjak, and Shibiao Bai. 2019. “Testing a New Ensemble Model Based on SVM and Random Forest in Forest Fire Susceptibility Assessment and Its Mapping in Serbia’s Tara National Park.” *Forests* 10(5):408.

Glenn, Edward P., Kiyomi Morino, Pamela L. Nagler, R. Scott Murray, Susanna Pearlstein, and

Kevin R. Hultine. 2012. “Roles of Saltcedar (Tamarix Spp.) and Capillary Rise in Salinizing a Non-Flooding Terrace on a Flow-Regulated Desert River.” *Journal of Arid Environments* 79:56–65.

Goetz, Jason N., Richard H. Guthrie, and Alexander Brenning. 2011. “Integrating Physical and Empirical Landslide Susceptibility Models Using Generalized Additive Models.” *Geomorphology* 129(3–4):376–86.

Golkarian, Ali, Seyed Amir Naghibi, Bahareh Kalantar, and Biswajeet Pradhan. 2018. “Groundwater Potential Mapping Using C5. 0, Random Forest, and Multivariate Adaptive Regression Spline Models in GIS.” *Environmental Monitoring and Assessment* 190(3):149.

Hastie, T. J. and R. J. Tibshirani. 1990. “Generalized Additive Models London Chapman and Hall.” *Inc*.

Hong, Haoyuan, Yamin Miao, Junzhi Liu, and A. Xing Zhu. 2019. “Exploring the Effects of the Design and Quantity of Absence Data on the Performance of Random Forest-Based Landslide Susceptibility Mapping.” *Catena* 176(December 2018):45–64.

Hong, Haoyuan, Seyed Amir Naghibi, Mostafa Moradi Dashtpagerdi, Hamid Reza Pourghasemi, and Wei Chen. 2017. “A Comparative Assessment between Linear and Quadratic Discriminant Analyses (LDA-QDA) with Frequency Ratio and Weights-of-Evidence Models for Forest Fire Susceptibility Mapping in China.” *Arabian Journal of Geosciences* 10(7):167.

Hong, Haoyuan, Mahdi Panahi, Ataollah Shirzadi, Tianwu Ma, Junzhi Liu, A. Xing Zhu, Wei Chen, Ioannis Kougias, and Nerantzis Kazakis. 2018. “Flood Susceptibility Assessment in Hengfeng

Area Coupling Adaptive Neuro-Fuzzy Inference System with Genetic Algorithm and Differential Evolution.” *Science of The Total Environment* 621:1124–41.

Janizadeh, Saeid, Mohammadtaghi Avand, Abolfazl Jaafari, Tran Van Phong, Mahmoud Bayat, Ebrahim Ahmadisharaf, Indra Prakash, Binh Thai Pham, and Saro Lee. 2019. “Prediction Success of Machine Learning Methods for Flash Flood Susceptibility Mapping in the Tafresh Watershed, Iran.” *Sustainability* 11(19):5426.

Kantakumar, Lakshmi N. and Priti Neelamsetti. 2015. “Multi-Temporal Land Use Classification Using Hybrid Approach.” *The Egyptian Journal of Remote Sensing and Space Science* 18(2):289–95.

Khosravi, Khabat, Binh Thai Pham, Kamran Chapi, Ataollah Shirzadi, Himan Shahabi, Inge Revhaug, Indra Prakash, and Dieu Tien Bui. 2018. “A Comparative Assessment of Decision Trees Algorithms for Flash Flood Susceptibility Modeling at Haraz Watershed, Northern Iran.” *Science of the Total Environment* 627(2):744–55.

Kordestani, Mojtaba Dolat, Seyed Amir Naghibi, Hossein Hashemi, Kourosh Ahmadi, Bahareh Kalantar, and Biswajeet Pradhan. 2019. “Groundwater Potential Mapping Using a Novel Data-Mining Ensemble Model.” *Hydrogeology Journal* 27(1):211–24.

Lee, Saro Sunmin, Jeong-Cheol Kim, Hyung-Sup Jung, Moung Jin Lee, and Saro Sunmin Lee. 2017. “Spatial Prediction of Flood Susceptibility Using Random-Forest and Boosted-Tree Models in Seoul Metropolitan City, Korea.” *Geomatics, Natural Hazards and Risk* 8(2):1185–1203.

Lee, Sunmin, Saro Lee, Moung-Jin Lee, and Hyung-Sup Jung. 2018. “Spatial Assessment of Urban Flood Susceptibility Using Data Mining and Geographic Information System (GIS) Tools.” *Sustainability* 10(3):648.

Maggini, Ramona, Anthony Lehmann, Niklaus E. Zimmermann, and Antoine Guisan. 2006. “Improving Generalized Regression Analysis for the Spatial Prediction of Forest Communities.” *Journal of Biogeography* 33(10):1729–49.

Motevalli, Alireza, Seyed Amir Naghibi, Hossein Hashemi, Ronny Berndtsson, Biswajeet Pradhan, and Vahid Gholami. 2019. “Inverse Method Using Boosted Regression Tree and K-Nearest Neighbor to Quantify Effects of Point and Non-Point Source Nitrate Pollution in Groundwater.” *Journal of Cleaner Production* 228:1248–63.

Motevalli, Alireza and Mehdi Vafakhah. 2016. “Flood Hazard Mapping Using Synthesis Hydraulic and Geomorphic Properties at Watershed Scale.” *Stochastic Environmental Research and Risk Assessment* 30(7):1889–1900.

Mousavi, Seyed Mohsen, Ali Golkarian, Seyed Amir Naghibi, Bahareh Kalantar, and Biswajeet Pradhan. 2017. “GIS-Based Groundwater Spring Potential Mapping Using Data Mining Boosted Regression Tree and Probabilistic Frequency Ratio Models in Iran.” *AIMS Geosci* 3(1):91–115.

Myint, Soe W., Patricia Gober, Anthony Brazel, Susanne Grossman-Clarke, and Qihao Weng. 2011. “Per-Pixel vs. Object-Based Classification of Urban Land Cover Extraction Using High Spatial Resolution Imagery.” *Remote Sensing of Environment* 115(5):1145–61.

Naghibi, Seyed Amir, Kourosh Ahmadi, and Alireza Daneshi. 2017. “Application of Support Vector Machine, Random Forest, and Genetic Algorithm Optimized Random Forest Models in Groundwater Potential Mapping.” *Water Resources Management* 31(9):2761–75.

Naghibi, Seyed Amir, Mojtaba Dolatkordestani, Ashkan Rezaei, Payam Amouzegari, Mostafa Taheri Heravi, Bahareh Kalantar, and Biswajeet Pradhan. 2019. “Application of Rotation Forest with Decision Trees as Base Classifier and a Novel Ensemble Model in Spatial Modeling of Groundwater Potential.” *Environmental Monitoring and Assessment* 191(4):248.

Naghibi, Seyed Amir and Mostafa Moradi Dashtpagerdi. 2016. “Evaluation of Four Supervised Learning Methods for Groundwater Spring Potential Mapping in Khalkhal Region (Iran) Using GIS-Based Features.” *Hydrogeology Journal* 1–21.

Naghibi, Seyed Amir and Hamid Reza Pourghasemi. 2015. “A Comparative Assessment Between Three Machine Learning Models and Their Performance Comparison by Bivariate and Multivariate Statistical Methods in Groundwater Potential Mapping.” *Water Resources Management* 29(14):5217–36.

Naghibi, Seyed Amir, Hamid Reza Pourghasemi, and Karim Abbaspour. 2018. “A Comparison between Ten Advanced and Soft Computing Models for Groundwater Qanat Potential Assessment in Iran Using R and GIS.” *Theoretical and Applied Climatology* 131(3–4):967–84.

Naghibi, Seyed Amir, Hamid Reza Pourghasemi, and Barnali Dixon. 2016. “GIS-Based Groundwater Potential Mapping Using Boosted Regression Tree, Classification and

Regression Tree, and Random Forest Machine Learning Models in Iran." *Environmental Monitoring and Assessment* 188(1):44.

Nandi, Arpita, Arpita Mandal, Matthew Wilson, and David Smith. 2016. "Flood Hazard Mapping in Jamaica Using Principal Component Analysis and Logistic Regression." *Environmental Earth Sciences* 75(6):465.

Ngo, Phuong-Thao, Nhat-Duc Hoang, Biswajeet Pradhan, Quang Nguyen, Xuan Tran, Viet Nguyen, Pijush Samui, and Dieu Tien Bui. 2018. "A Novel Hybrid Swarm Optimized Multilayer Neural Network for Spatial Prediction of Flash Floods in Tropical Areas Using Sentinel-1 SAR Imagery and Geospatial Data." *Sensors* 18(11):3704.

Nourani, Vahid and Mehdi Komasi. 2013. "A Geomorphology-Based ANFIS Model for Multi-Station Modeling of Rainfall–Runoff Process." *Journal of Hydrology* 490:41–55.

Nourani, Vahid, Biswajeet Pradhan, Hamid Ghaffari, and Seyed Saber Sharifi. 2014. "Landslide Susceptibility Mapping at Zonouz Plain, Iran Using Genetic Programming and Comparison with Frequency Ratio, Logistic Regression, and Artificial Neural Network Models." *Natural Hazards* 71(1):523–47.

Pal, Mahesh. 2005. "Random Forest Classifier for Remote Sensing Classification." *International Journal of Remote Sensing* 26(1):217–22.

Petschko, H., A. Brenning, R. Bell, J. Goetz, and T. Glade. 2014. "Assessing the Quality of Landslide Susceptibility Maps–Case Study Lower Austria." *Natural Hazards and Earth System Sciences* 14(1):95–118.

Pourtaghi, Zohre Sadat, Hamid Reza Pourghasemi, Roberta Aretano, and Teodoro Semeraro. 2016. “Investigation of General Indicators Influencing on Forest Fire and Its Susceptibility Modeling Using Different Data Mining Techniques.” *Ecological Indicators* 64:72–84.

Rahmati, Omid, Seyed Amir Naghibi, Himan Shahabi, Dieu Tien Bui, Biswajeet Pradhan, Ali Azareh, Elham Rafiei-Sardooi, Aliakbar Nazari Samani, and Assefa M. Melesse. 2018. “Groundwater Spring Potential Modelling: Comprising the Capability and Robustness of Three Different Modeling Approaches.” *Journal of Hydrology* 565:248–61.

Rahmati, Omid and Hamid Reza Pourghasemi. 2017. “Identification of Critical Flood Prone Areas in Data-Scarce and Ungauged Regions: A Comparison of Three Data Mining Models.” *Water Resources Management* 31(5):1473–87.

Rahmati, Omid, Hamid Reza Pourghasemi, and Hossein Zeinivand. 2016. “Flood Susceptibility Mapping Using Frequency Ratio and Weights-of-Evidence Models in the Golastan Province, Iran.” *Geocarto International* 31(1):42–70.

Sahoo, G. B., C. Ray, and E. H. De Carlo. 2006. “Use of Neural Network to Predict Flash Flood and Attendant Water Qualities of a Mountainous Stream on Oahu, Hawaii.” *Journal of Hydrology* 327(3–4):525–38.

Sameen, Maher Ibrahim, Biswajeet Pradhan, and Saro Lee. 2019. “Self-Learning Random Forests Model for Mapping Groundwater Yield in Data-Scarce Areas.” *Natural Resources Research* 28(3):757–75.

Sangchini, Ebrahim Karimi, Seyed Naim Emami, Naser Tahmasebipour, Hamid Reza

Pourghasemi, Seyed Amir Naghibi, Seyed Abdolhossein Arami, and Biswajeet Pradhan. 2016. “Assessment and Comparison of Combined Bivariate and AHP Models with Logistic Regression for Landslide Susceptibility Mapping in the Chaharmahal-e-Bakhtiari Province, Iran.” *Arabian Journal of Geosciences* 9(3):201.

Shafapour, Mahyat, Tehrany Biswajeet, Mahyat Shafapour Tehrany, Biswajeet Pradhan, and Mustafa Neamah Jebur. 2015. “Flood Susceptibility Analysis and Its Verification Using a Novel Ensemble Support Vector Machine and Frequency Ratio Method.” *Stochastic Environmental Research and Risk Assessment* 29(4):1149–65.

Shin, Ju-Young, Yonghun Ro, Joo-Wan Cha, Kyu-Rang Kim, and Jong-Chul Ha. 2019. “Assessing the Applicability of Random Forest, Stochastic Gradient Boosted Model, and Extreme Learning Machine Methods to the Quantitative Precipitation Estimation of the Radar Data: A Case Study to Gwangdeoksan Radar, South Korea, in 2018.” *Advances in Meteorology* 2019(Ml).

Tehrany, M. S., M. J. Lee, B. Pradhan, M. N. Jebur, and S. Lee. 2014. “No Title.” *Environ Earth Sci* 72(null):4001.

Tehrany, Mahyat Shafapour, Simon Jones, and Farzin Shabani. 2019. “Identifying the Essential Flood Conditioning Factors for Flood Prone Area Mapping Using Machine Learning Techniques.” *Catena* 175:174–92.

Tehrany, Mahyat Shafapour, Biswajeet Pradhan, and Mustafa Neamah Jebur. 2013. “Spatial Prediction of Flood Susceptible Areas Using Rule Based Decision Tree (DT) and a Novel Ensemble Bivariate and Multivariate Statistical Models in GIS.” *Journal of Hydrology* 504.

Termeh, Seyed Vahid Razavi, Aiding Kornejady, Hamid Reza Pourghasemi, and Saskia Keesstra. 2018. “Flood Susceptibility Mapping Using Novel Ensembles of Adaptive Neuro Fuzzy Inference System and Metaheuristic Algorithms.” *Science of the Total Environment* 615:438–51.

Thakkar, Amee K., Venkappayya R. Desai, Ajay Patel, and Madhukar B. Potdar. 2017. “Post-Classification Corrections in Improving the Classification of Land Use/Land Cover of Arid Region Using RS and GIS: The Case of Arjuni Watershed, Gujarat, India.” *The Egyptian Journal of Remote Sensing and Space Science* 20(1):79–89.

Tien Bui, Dieu, Biswajeet Pradhan, Haleh Nampak, Quang-Thanh Bui, Quynh-An Tran, and Quoc-Phi Nguyen. 2016. “Hybrid Artificial Intelligence Approach Based on Neural Fuzzy Inference Model and Metaheuristic Optimization for Flood Susceptibilitgy Modeling in a High-Frequency Tropical Cyclone Area Using GIS.” *Journal of Hydrology* 540:317–30.

Tien, Dieu, Paraskevas Tsangaratos, Phuong-Thao Thi Ngo, Tien Dat, Binh Thai, Dieu Tien Bui, Paraskevas Tsangaratos, Phuong-Thao Thi Ngo, Tien Dat Pham, and Binh Thai Pham. 2019. “Flash Flood Susceptibility Modeling Using an Optimized Fuzzy Rule Based Feature Selection Technique and Tree Based Ensemble Methods.” *Science of The Total Environment* 668:1038–54.

Vorpahl, Peter, Helmut Elsenbeer, Michael Märker, and Boris Schröder. 2012. “How Can Statistical Models Help to Determine Driving Factors of Landslides ?” *Ecological Modelling* 239:27–39.

Wan, Sa, TCb Lei, and TYc Chou. 2010. “A Novel Data Mining Technique of Analysis and

Classification for Landslide Problems.” *Natural Hazards* 52(1):211.

Wang, Yi, Haoyuan Hong, Wei Chen, Shaojun Li, Dragan Pamučar, Ljubomir Gigović, Siniša Drobnjak, Dieu Tien Bui, and Hexiang Duan. 2019. “A Hybrid GIS Multi-Criteria Decision-Making Method for Flood Susceptibility Mapping at Shangyou, China.” *Remote Sensing* 11(1):62.

Yousefi, S., H. R. Moradi, H. R. Pourghasemi, and R. Khatami. 2017. “Assessment of Floodplain Landuse and Channel Morphology within Meandering Reach of the Talar River in Iran Using GIS and Aerial Photographs.” *Geocarto International* 6049(September):1–14.

Youssef, Ahmed M., Biswajeet Pradhan, and Abdallah Mohamed Hassan. 2011. “Flash Flood Risk Estimation along the St. Katherine Road, Southern Sinai, Egypt Using GIS Based Morphometry and Satellite Imagery.” *Environmental Earth Sciences* 62(3):611–23.

Zhao, Gang, Bo Pang, Zongxue Xu, Dingzhi Peng, and Liyang Xu. 2019. “Assessment of Urban Flood Susceptibility Using Semi-Supervised Machine Learning Model.” *Science of The Total Environment* 659:940–49.

Zhao, Gang, Bo Pang, Zongxue Xu, Jiajia Yue, and Tongbi Tu. 2018. “Mapping Flood Susceptibility in Mountainous Areas on a National Scale in China.” *Science of The Total Environment* 615:1133–42.